J. Min. Metall. Sect. B-Metall. 55 (2) B (2019) 177 - 185

Journal of Mining and Metallurgy, Section B: Metallurgy

REDUCTION BEHAVIOR OF Tin-CONTAINING PHASE IN Tin-BEARING IRON CONCENTRATES UNDER CO-CO_2 MIXED GASES

Y. Yu [a], H.-J. Li [*a,b], L. Li [a]

[a*] State Key Laboratory of Complex Non-ferrous Metal Resources Clean Utilization, Engineering Research Center of Metallurgical Energy Conservation and Emission Reduction of Ministry of Education, Faculty of Metallurgical and Energy Engineering, Kunming University of Science and Technology, Kunming, China
[b] Quality Development Institute, Kunming University of Science and Technology, Kunming, China

(Received 21 November 2018; accepted 26 March 2019)

Abstract

The main purpose of this study was to ascertain the reduction behavior of tin phase (SnO_2) in tin-bearing iron concentrates at the respective temperature of 1273 and 1373 K in diverse CO-CO_2 mixed gases using chemical analysis, XRD, and SEM-EDS analysis. The results show that the reduction behavior of SnO_2 depends on the roasting temperature and CO content. At 1273 K, the SnO_2 will be reduced to Sn (l) with the CO content being higher than 17.26 vol%, and there is no formation of SnO(s). With the temperature increased to 1373 K, the SnO_2 is reduced stepwise in the order to form SnO_2 → SnO (l) → Sn(l) with CO content over 15.75 vol%. The kinetic study shows that activation energy of the reaction $SnO_2(s)+CO(g)=Sn(l)+CO_2(g)$ is 144.75 kJ/mol at 1073-1223 K, being far lower than the one in the reduction of $SnO_2(s)$ into SnO(g) at 1273-1323 K, which leads to a conclusion that the tin in tin-bearing iron concentrates could be removed effectively after the Sn(l) sulfurated into SnS at relatively lower temperatures (1073-1223 K) using the sulfidation roasting method.

Keywords: *Reduction behavior; SnO_2; CO-CO_2 mixed gases; Kinetics; Tin-bearing iron concentrates*

1. Introduction

There is a typical iron ore containing tin with the total reserve of more than 0.5 billion tons in China, which is mainly found in Neimenggu, Guangxi, Hunan, and Yunnan provinces of China [1-3]. After these tin-bearing iron ores were treated by joint processes of reselection, magnetic separation and flotation, the Fe content reached up to 60% while the tin content was about 0.3-0.8 wt.% in the tin-bearing iron concentrates. The tin impurity can make steel crisp, and it cannot be used for iron-making when the tin content is in excess of 0.08 wt. % [4,5]. Previous studies shows iron and tin in the tin-bearing iron concentrates exist mainly in forms of magnetite (Fe_3O_4) and cassiterite (SnO_2), and the Sn phase is almost embedded in the iron phase (Fe_3O_4) at fine-grained size, resulting that recovery of tin is low by mineral processing methods [6]. The tin could be separated efficiently through the methods of reduction or sulfidation roasting processes [6-16]. Reductant is used in many metallurgical processes to control oxygen potential of the reaction system [17]. Using CO as the reductant, for the reduction roasting process, the Sn phase (SnO_2) is reduced and further removed in the form of gaseous SnO, through which the tin content in the iron concentrate can decrease to 0.08 wt.% with the original tin content being below 0.35 wt.% in the tin-bearing iron concentrates [11-12]. The sulfidation roasting process takes place at a higher rate at the point of Sn removal than the reduction roasting process when the Sn content in the tin-bearing iron concentrate is relatively high, in which the tin volatilization rate reaches over 90% using the FeS_2 or high sulfur coal [8-9]. In this process, the SnO_2 is reduced firstly and then sulfurized and removed by gaseous SnS. The reduction of SnO_2 is the joint pathway in these two roasting methods.

The detailed reduction behavior of SnO_2 have been mainly conducted by Zhang and Tao, and there are some big discrepancies between their reports [12,16]. Tao reported the reduction behavior of SnO_2 is mainly related to roasting temperature. When the

*Corresponding author: 252972286@qq.com

DOI:10.2298/JMMB181121025Y

roasting temperature increased from 1073 K to 1313 K, SnO_2 was reduced to SnO(s) and then transformed to Sn(l) and SnO_2 through the disproportionation of SnO. For temperature at 1313 K, SnO_2 was firstly reduced to SnO(l) and then to Sn(l). However, Zhang believed that the reduction behavior of SnO_2 was also related to the CO content in the CO-CO_2 mixed gases beside the roasting temperature. Under relatively weak reductive atmosphere, the SnO_2 was firstly reduced to SnO(s) and then to Sn(l) in the temperature range of 1073 K-1473 K, and the disproportionation of SnO did not occur. Meanwhile there was no generation of SnO(l) with roasting temperature reaching to 1313 K. As CO content further increased, SnO_2 was reduced directly to Sn (l) in the temperature range of 1073 K- 1473 K. In addition, it should be noted that it was not proved whether the intermediate product SnO(s,l) was formed in Tao and Zhang researches.

Consequently, isothermal reduction tests of SnO_2 were performed in this paper with the assistance of chemical analysis, XRD, and SEM-EDS analysis under different CO/CO_2 gas mixtures, aiming to study the reduction behavior of SnO_2. Meanwhile, isothermal reduction kinetics of reduction SnO_2 was performed in a 30 vol% CO-70 vol% CO_2 atmosphere, aiming to provide theoretical guideline for the tin removal using sulfidation roasting method.

2. Experimental

2.1. Materials

The SnO_2, SiO_2, and Fe powders were used in this study, which were analytical purity chemical reagent from Tianjin Shentai Chemical Reagent Technology Co. Ltd., China. The SnO_2 powder was analyzed with X-ray fluorescence spectroscopy (XRF), and detailed result is shown in Table 1. CO (purity 99.99 vol %), CO_2 (purity 99.99 vol %), and N_2 (purity 99.999 vol%), were used as the reducing gas and the shielding gas, respectively.

Table 1. *Composition of the SnO_2 powders (wt%)*

Element	SnO_2	Fe	Pb	Ni
Content	99.8480	0.0717	0.0634	0.0169

2.2. Experimental apparatus and Procedure

The experimental device is shown in Fig.1, in which the temperature control accuracy was ± 1K using an intelligent temperature controller. The mass flow controllers with a minimum scale division of 0.1 ml/min were used to control CO and CO_2 contents in the mixed gases.

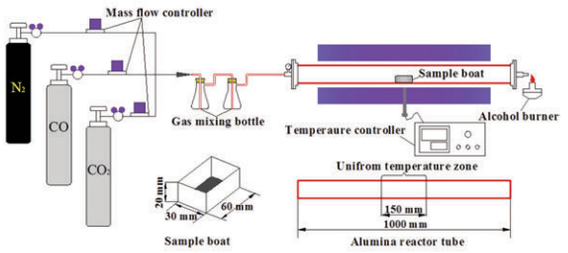

Figure 1. *The schematic of the experimental apparatus*

All the experiments were carried out in an alumina sample boat which holds the samples as shown in Fig.1. For the experimental procedure, the alumina sample boat was firstly heated to the desired temperature, and then high-purity N_2 was blown into the alumina reactor tube for 15 min to purge the air. Secondly, for each test, 0.80 g of the samples, which had been ground to 200 μm, were put into the electric furnace in a gas mixture of CO and CO_2. After the reduction roasting, the roasted product was rapidly taken out and quenched into liquid nitrogen. Finally, the product was weighed and kept in a closed vessel for analysis.

The tin content in the roasted residue was analyzed by chemical analysis, and the volatilized fraction of it was calculated in accordance with the following expression:

$$R = \left[1-\left(m_1 w_{1,Sn} / m_0 w_{0,Sn}\right)\right]\times 100\ \%$$

Where, R is the tin volatilized fraction, %; m_0 is the mass of the original sample, g; m_1 is the mass of the roasted residue, g; $w_{0,\,Sn}$ is the tin content of the original sample; $w_{1,Sn}$ is the tin content of the roasted residue.

The Gibbs free energy changes (△G) in this paper were calculated using the reaction module of FactSage7.0. The phase compositions of roasted residues were examined by XRD patterns using a Japan Science D/max-R diffractometer with Cu Kα radiation (λ=1.5406 Å), operating voltage of 40 kV, and current of 40 mA. The diffraction angle (2θ) was scanned from 10 to 90 deg. The microstructure of roasted residues was determined by scanning electron microscopy (SEM; HITACHI-S3400N) coupled with energy dispersive X-ray spectroscopy (EDS).

3. Thermodynamic analyses

The Sn-O-C equilibrium diagram could be summarized in Fig.2 based on the previous research [12]. The SnO_2 is reduced to SnO(s) (Eq. (1)), and then volatilized as SnO (g) (Eq. (4)) in the area B, and the SnO(s) is further reduced to Sn (l) (Eq. (2)) increasing CO content to the area C. In the area D, the reaction (3) takes place, and the tin volatilization occurs through reactions (4) and (5).

$$SnO_2(s)+CO(g)=SnO(s)+CO_2(g) \quad (1)$$

$$SnO(s)+CO(g)=Sn(l)+CO_2(g) \quad (2)$$

$$SnO_2(s)+2CO(g)=Sn(l)+2CO_2(g) \quad (3)$$

$$SnO(s)=SnO(g) \quad (4)$$

$$SnO_2(s)+Sn(l)=2SnO(s) \quad (5)$$

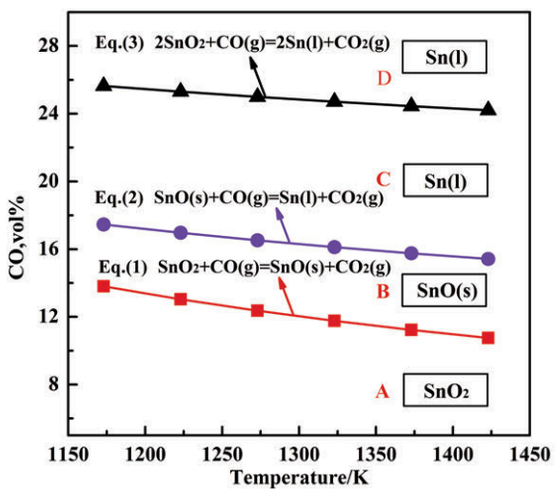

Figure 2. *Gas-equilibrium diagram of Sn-O-C system by [12]*

However, the O-Sn phase diagram [18] (Fig.3) shows that the Sn(l) is in equilibrium with SnO_2(s) when the temperature is at 729 K-1313 K, indicating that the reduction of SnO_2 was a one-step reaction, SnO_2(s)→Sn(l). The SnO(l) is found in equilibrium

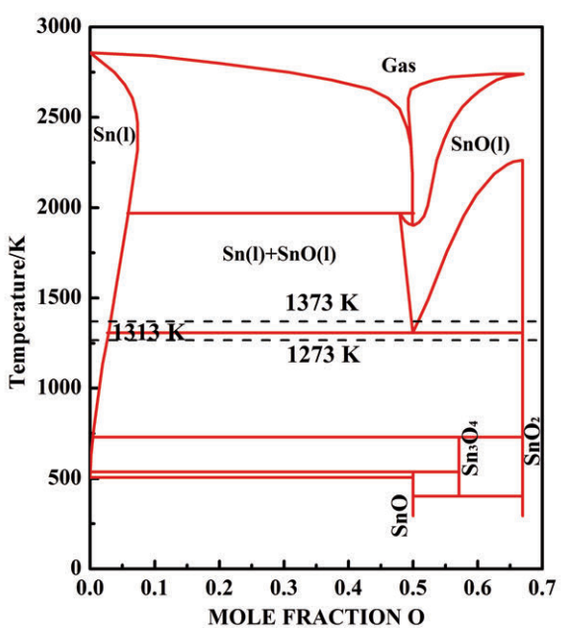

Figure 3. *O–Sn phase diagram, calculated at 1 bar*

with Sn(l) and SnO_2(s) increasing temperature over 1313K, indicating that the reduction of SnO_2 was a step-by-step process, SnO_2 (s)→SnO(l)→Sn(l). Based on the O-Sn phase diagram, the gas-equilibrium diagram of Sn-O-C system could be drawn as shown in Fig.4. Combined with the discrepancy between Fig.2 and Fig.3, the reduction behavior of SnO_2 will be discussed in this paper at temperature of 1273 K and 1373 K respectively in diverse CO-CO_2 mixed gases as shown in Fig.4.

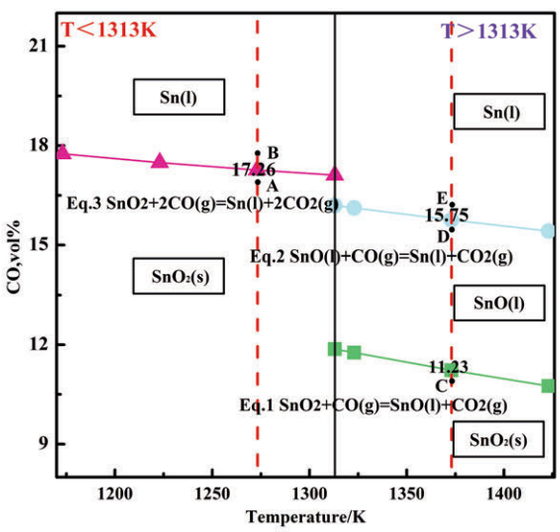

Figure 4. *Gas-equilibrium diagram of Sn-O-C system*

4. Results and discussion

4.1. Reduction and volatilization behaviors of SnO_2

Based on the difference in thermodynamic, the CO contents at the points of A (17.00 vol% CO) and B (17.50 vol% CO) in Fig.4 were chosen for studying the SnO_2 reduction behavior under CO-CO_2 mixed gases total flow rate of 500 ml/min, roasting temperature of 1273 K and residence time of 180 min.

Fig.5 shows that the main phase of roasted residues is SnO_2 at the CO content of 17.00 vol%, and 17.50 vol% respectively. Though the Sn (l) could be generated thermodynamically in Fig.4, it can't be detected in sample B (17.50 vol% CO). Besides, SnO (s) is not generated in sample A (17.00 vol% CO), as can be seen in Fig.5 which is in accordance with the thermodynamic analysis in Fig.4. In order to further investigate whether SnO(s) and Sn(l) were generated in samples A (17.00 vol% CO) and B (17.50 vol% CO) respectively, equivalent mole SiO_2 or Fe were added, blended with SnO_2 and then roasted at 1273 K for 180 min in 17.00 vol% and 17.50 vol% CO respectively.

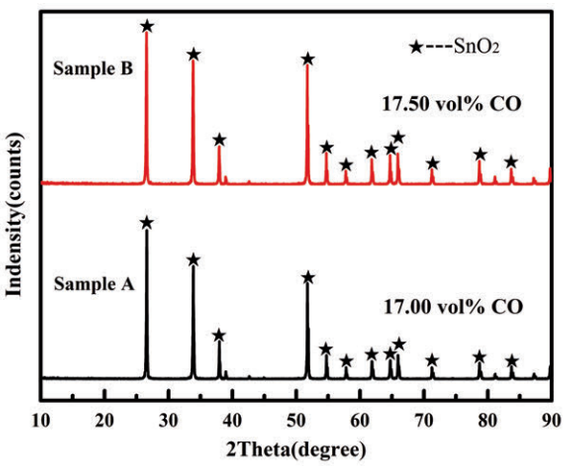

Figure 5. *XRD patterns of roasted residues of SnO_2 at 1273 K in different CO contents*

The SEM-EDS results of the roasted residues in CO contents of 17.00 vol% and 17.50 vol% are shown in Fig.6 and Fig.7 respectively. The SEM image in Fig.6 reveals two distinct regions appearing with different brightness, and the EDS results of regions 1 and 2 show that the dark gray and bright regions are SiO_2 and SnO_2 respectively, indicating that there is no formation of SnO(s) with the CO content of 17.00 vol%. The region 1 in Fig.7 is made up of predominant elements of Sn, Si, Al and O, which implies that a tin-bearing silicate is formed [19-20]. The Al element detected in the silicate is due to contamination of the melts from the sample boat during the roasting process [20]. According to Fig.4, this tin in the tin-bearing silicate may be derived from Sn(l) which comes from the reduction of SnO_2, and then it reacted with SnO_2(s) forming SnO and further formed the tin-bearing silicate with SiO_2. Namely, a mixed sample of SnO_2 and equivalent mole Fe was roasted for 180 min at 1273 K in CO content of 17.50 vol% and SEM-EDS of this residue is shown in Fig.8. Fig.8 shows that the phase of region 1 is made up of Sn and Fe, indicating that there is a newborn metallic tin generated during the roasting process, which corresponds well with the results in Fig.4. In this process, the SnO_2 can be reduced to Sn (l) directly at 1273 K.

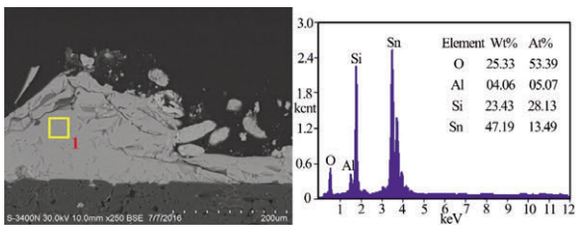

Figure 7. *SEM-EDS of the roasted residue of SnO_2 and SiO_2 roasted at 1273 K in CO content of 17.50 vol% for 180 min*

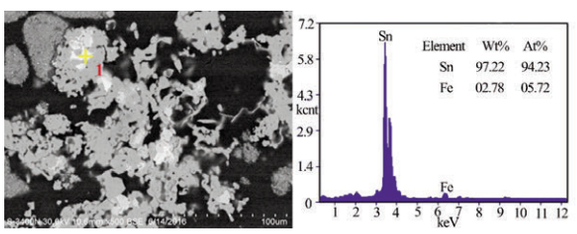

Figure 8. *SEM-EDS of the roasted residue of SnO_2 and Fe roasted at 1273 K in CO content of 17.50 vol% for 180 min*

Similar to the research at 1273 K, three CO contents of C(10.80 vol%), D (15.25 vol%), and E (16.15 vol%) in Fig.4 were chosen for studying the reduction behavior of SnO_2 under total CO-CO_2 mixed gases flow rate of 500 ml/min, roasting temperature of 1373 K, and residence time of 60 min.

Fig.9 shows that when the CO content increases from 10.80 vol% to 16.15 vol%, the main phase of roasted residues is always SnO_2. Combined with Fig.4, some tests were performed to investigate whether SnO(l) is generated in sample D. The SnO_2 was blended with equivalent mole SiO_2 and then roasted at 1373 K for 60 min in 10.80 vol% and 15.25 vol% CO contents respectively. The SEM-EDS results of roasted residues are shown in Figs.10 and 11 respectively. With the CO content of 10.80 vol%, there are two different regions of dark and light gray in Fig.10, which are SiO_2 and SnO_2 respectively. When the CO content is 15.25 vol%, the regions of 1 and 2 in Fig.11 consist of the predominant elements of Sn, Si, Al and O, meaning a tin-bearing silicate is generated. According to Fig.4, the tin in this tin-bearing silicate is derived from SnO(l). The SnO_2 is

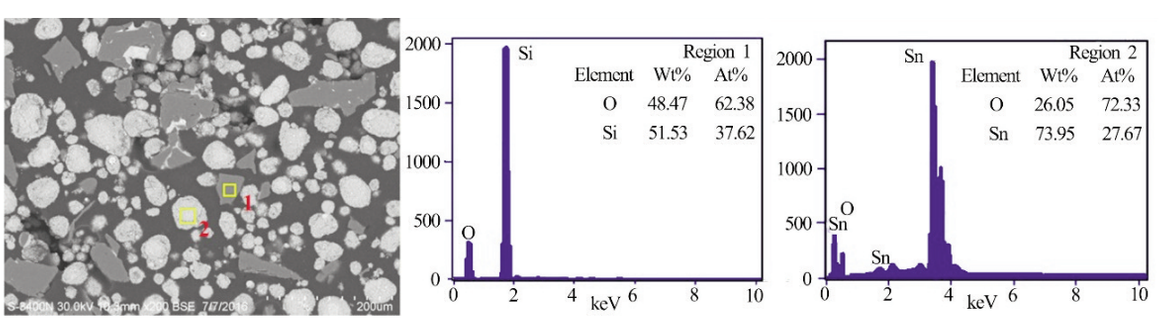

Figure 6. *SEM-EDS of the roasted residue of SnO_2 and SiO_2 roasted at 1273 K in CO content of 17.00 vol% for 180 min*

reduced stepwise in the order of SnO_2 → SnO (l) → Sn(l) at 1373 K.

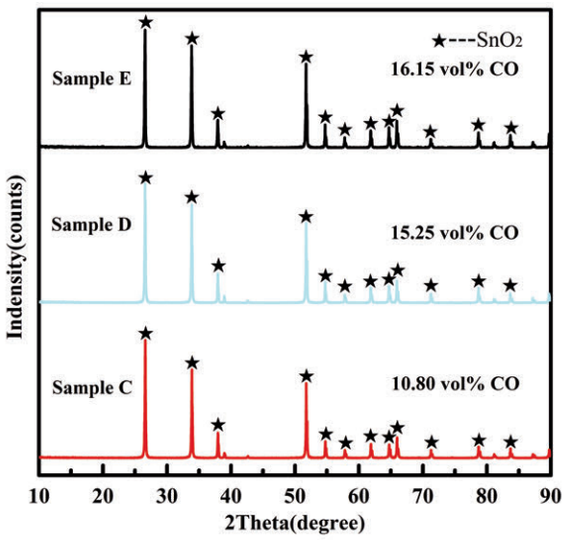

Figure 9. *XRD patterns of the roasted residues of SnO_2 at 1373 K and different CO volume fractions*

According to obtained results, the SnO_2 could not be reduced when the CO content was lower than 17.26 vol% at 1273 K and 11.23 vol% at 1373 K respectively, and tin volatilized fraction should not be observed. However, as presented in Fig.12, the tin volatilized fraction changes from 1.06 wt. % to 6.27 wt. % in the CO content from 8.00 vol% to 17.00 vol% at 1273 K, and the tin volatilized fraction is 4.25 wt. % at 8.00 vol% CO content at 1373 K. It might be attributed to the direct formation of gaseous SnO(g) (Eq. (6)). Fig.13 shows that the Eq. (6) can proceed by decreasing the SnO(g) partial pressure ($P_{SnO(g)}$) and increasing temperature. The SnO(g) partial pressure is low and always decreasing in the roasting process due to its strong volatility, and it can be removed effectively under relatively weak reductive atmosphere.

$$SnO_2(s)+CO(g)=SnO(g)+CO_2(g) \quad (6)$$

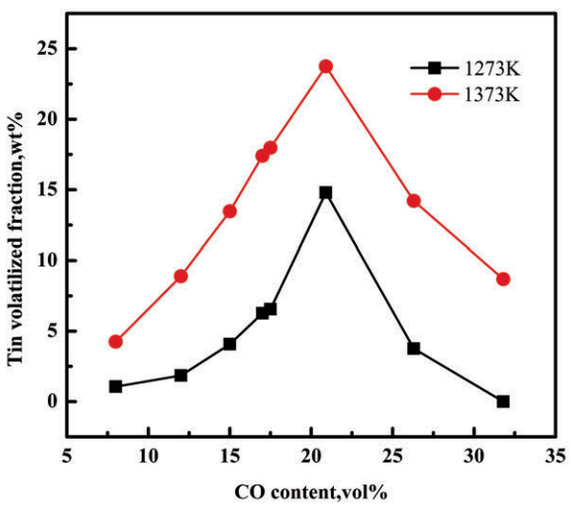

Figure 12. *Effect of CO content on the tin volatilized fraction*

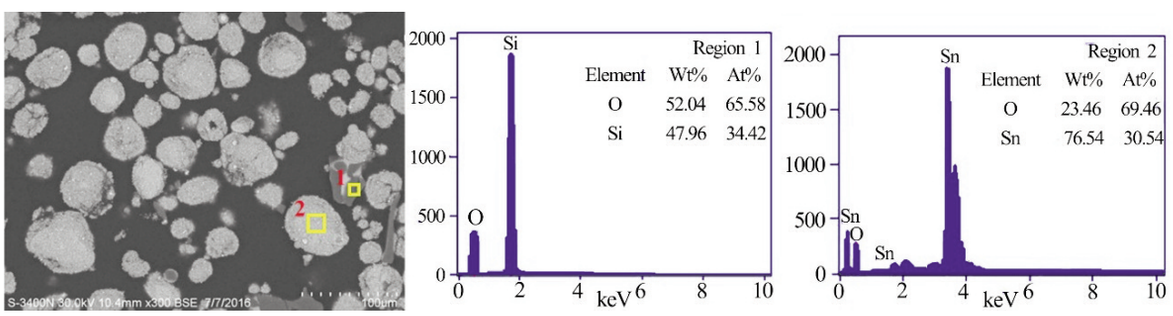

Figure 10. *SEM-EDS of the roasted residue of SnO_2 and SiO_2 roasted at 1373 K in CO content of 10.80 vol% for 60 min*

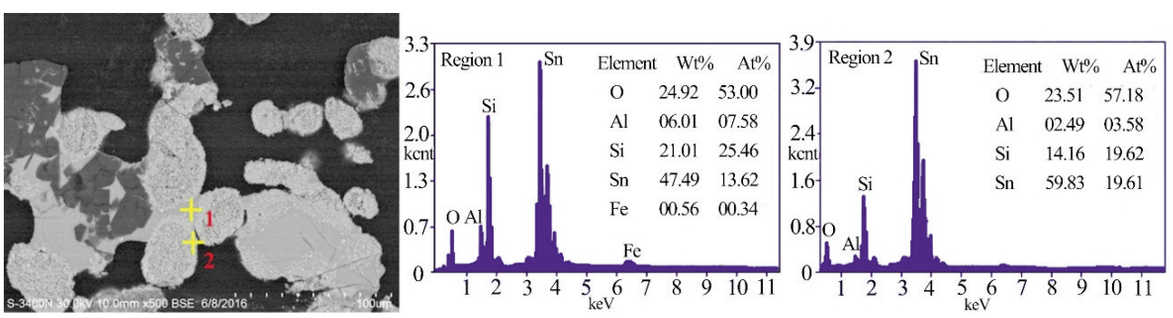

Figure 11. *SEM-EDS of the roasted residue of SnO_2 and SiO_2 roasted at 1373 K in CO content of 15.25 vol% for 60 min*

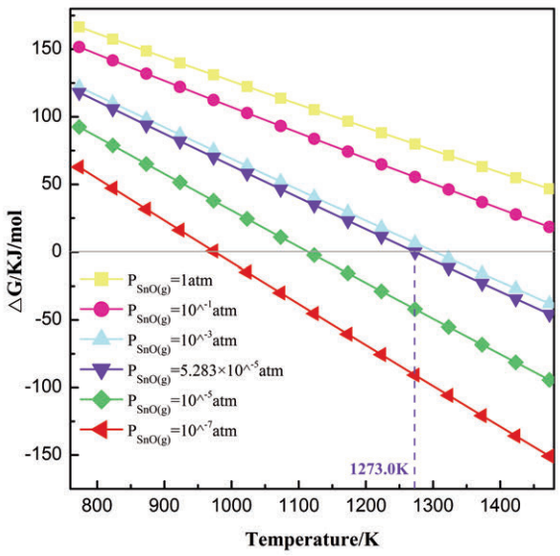

Figure 13. *Gibbs free energy changes of Eq. (6) with temperature under different* $P_{SnO(g)}$

In order to obtain high tin volatilized fraction, the reduction process should be conducted at a higher temperature, but this accelerates the formation of fayalite which reduces the quality of iron ore. Zhang reported that the optimal temperature range for removing tin from tin-bearing iron concentrates by reduction roasting is 1273-1323 K [11]. Table 2 shows that the vapor pressure of SnS at 1073-1223 K is similar to that of SnO at 1273-1373 K, so the tin might be removed in the form of SnS at a relatively low temperature with sulfidation roasting process. In addition, the reaction of Eq.(3) occupies a dominant place in the sulfidation roasting process, which is different from that in the reduction process.[8,12] Consequently, it was necessary to study the kinetic parameters of Eq.(3).

4.2 Kinetics of the reduction of SnO_2 to Sn(l) in the sulfidation roasting process

In the temperature range of 1073-1223 K, time range of 5-80 min, CO content range of 30.0-80.0 vol%, and gas total flow rate ($CO+CO_2$) of 500 mL/min, the SnO_2 powders were isothermally reduced. The tin contents in the roasted residues in different experimental states are shown in Table 3 and Table 4.

Table 3. *Effect of temperature on the Sn residual content in 30 vol% CO content (wt%)*

	Sn content			
Temperature/K	1073 K	1123 K	1173 K	1223 K
5 min	79.34	80.33	83.17	84.44
10 min	79.99	82.18	84.17	86.74
15 min	80.91	84.55	87.33	93.68
20 min	81.30	86.02	90.84	96.65
30 min	/	89.43	96.22	98.97
40 min	83.98	92.19	99.02	/
60 min	88.28	/	/	/
80 min	91.48	/	/	/

Table 4. *Effect of CO content on the Sn residual content at 1123 K (wt%)*

	Sn content					
CO content	30 vol%	40 vol%	50 vol%	60 vol%	70 vol%	80 vol%
5 min	80.33	82.77	85.09	88.41	90.24	91.93
7.5 min	/	/	/	/	94.01	95.56
10 min	82.18	85.72	89.47	94.07	96.49	97.69
12.5 min	/	/	/	/	98.02	98.82
15 min	84.55	89.29	92.86	97.91	/	/
20 min	86.02	92.54	96.20	99.30	/	/
30 min	89.43	95.26	/	/	/	/
40 min	92.19	/	/	/	/	/

According to the previous references [21], the nucleation and growth model was chosen to describe the kinetic characteristics of Eq.(3). The corresponding kinetic equation is presented as Eq. [7]

$$\left[-ln\left(1-X_{SnO2}\right)\right]^{1/m} = k_{app} \times t \tag{7}$$

where X_{SnO2} is the reduction ratio of SnO_2, m is a constant, t is the reaction time (min), and kapp is the apparent rate constant (min^{-1}) which could be obtained by Eq. (8)

$$k_{app} = b \times k \times f\left(p_{co}\right) = b \times k \times {p_{co}}^{n} \tag{8}$$

where b stands for the stoichiometry constant and equals to 1/2 in this system deduced from Eq.(3), k for

Table 2. *The vapor pressure of SnO and SnS*

Temperature/K	1073	1123	1173	1223	1273	1323	1373	1423
P_{SnO}^{Θ}	4.31	15.15	47.87	137.64	364.28	895.68	2062.6	4479.5
P_{SnS}^{Θ}	257.0	674.7	1631	3668.1	7740.5	15438	29281	53091

the intrinsic rate constant ($min^{-1}\cdot kPa^{-n}$), f for the partial pressure dependence of the rate, pco for the CO partial pressure (kPa), and n for the reaction order. When using ln[-ln(1-X_{SnO2})] as Y- axis and ln t as X-axis, there is a linear relationship between X and Y, and the slope of the line is m.

The experimental data were processed in Table 3 and Table 4 using the kinetic Eq. (7) and plotted in Figs.14 and 15 with a regression analysis. Examination of these figures reveals that the rate data follows Eq. (7) well. With totaling nine runs, the best-fit values of m in Fig.14 and Fig.15 vary between 1.05 and 1.20. The use of a single value of m for the same material is in accordance with the mechanistic justification of the use of the nucleation and growth kinetics equation, and thus all of the calculated lines were plotted with an average value of m being 1.14.

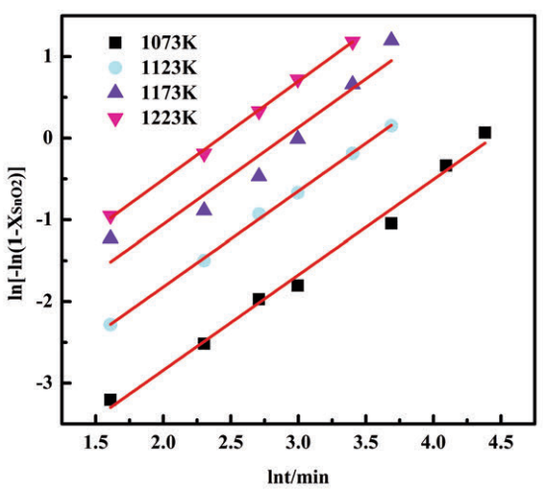

Figure 14. *Plots of ln[-ln(1-X_{SnO2})] versus ln t at different temperatures using the rate data of Table 3 according to Eq. (7)*

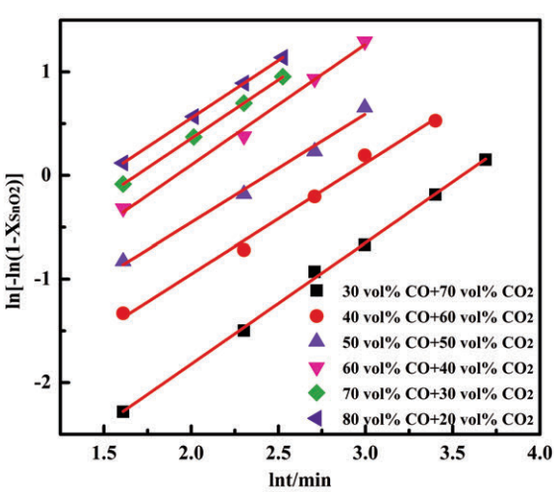

Figure 15. *Plots of ln[-ln(1-X_{SnO2})] versus ln t at different CO contents using the rate data of Table 4 according to Eq. (7)*

The values of k_{app} against the CO partial pressure obtained from the intercepts are plotted in Fig. 16, which shows a straight line that goes through the origin. It indicates a first-order reaction with respect to the CO partial pressure. Thus, Eq. (8) can be abbreviated as Eq. (9)

$$k_{app} = b \times k \times f(p_{CO}) = 1/2 \times k \times p_{CO} \quad (9)$$

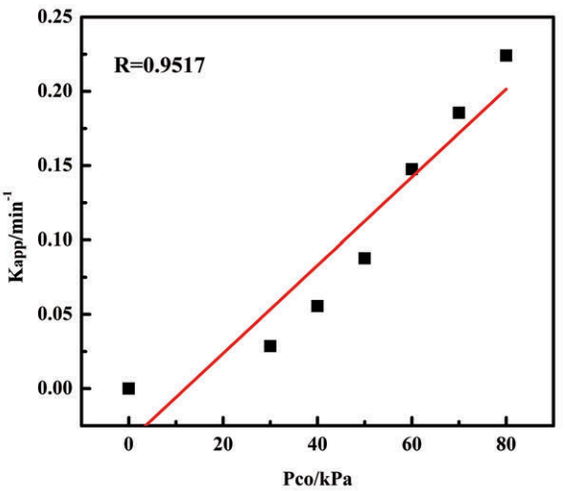

Figure 16. *Values of the apparent reaction rate constant against CO partial pressure based on the results in Table 4*

The values of the rate constant at various temperatures, k obtained from Eq. (9), were plotted in Fig. 17. The slope of the straight line placed through the experimental points in Fig.17 corresponds to the activation energy of 144.75 kJ/mol.

Zhang [12] reported that the tin could be removed

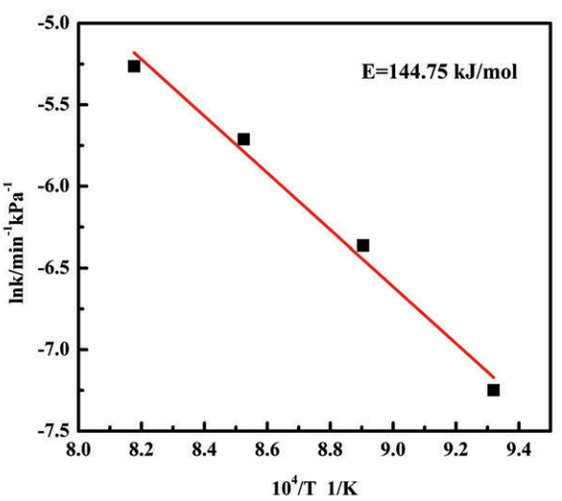

Figure 17. *Arrhenius plot of the intrinsic rate constants obtained from the results of Table 3*

effectively at 1273-1323 K in the CO content range of 15.0 vol%-16.25 vol%, and Eq.(6) holds a dominant position in their roasting process according to Fig.4 and Fig.13. The activation energy of Eq.(6) changed from 328.79 kJ/mol at CO 10.0% to 248.13 kJ/mol at CO 12.5% [22],which is far higher than that of Eq.(3) at 1073 -1223 K in CO content range of 30.0 vol%. It leads to a conclusion that the tin in tin-bearing iron concentrates could be removed effectively after the Sn(l) is sulfurated into SnS at relatively lower temperatures (1073-1223 K) using the sulfidation roasting method.

5. Conclusions

The reduction behavior of SnO_2 under different temperatures was studied in this paper. From the findings, the following conclusions were obtained.

1. The reduction behavior of SnO_2 at 1273 K depends on the CO content, which is different from the previous study. The reaction of $SnO_2(s)+CO(g)=SnO(g)+CO_2(g)$ proceeds in arbitrary content of CO at 1273 K. When CO content is higher than 17.26 vol%, the SnO_2 is reduced to Sn(l) directly, and the generated Sn(l) can react with SnO_2(s) and form SnO.

2. The reaction of $SnO_2(s)+CO(g) = SnO(g)+CO_2(g)$ also proceeds in arbitrary content of CO at 1373 K. Different from that at 1273 K, when CO content is higher than 15.25 vol%, the SnO_2 is reduced to SnO(l) firstly, and then the generated SnO(l) can be further reduced to Sn(l) at a higher CO content.

3. The activation energy of the reaction $SnO_2(s)+CO(g)=Sn(l)+ CO_2(g)$ is far lower than that in the reduction of SnO_2(s) into SnO(g). The tin in the tin-bearing iron concentrates could be removed effectively after the Sn(l) being transformed into SnS at relatively lower temperatures (1073-1223 K) using the sulfidation roasting method.

Acknowledgement

The authors wish to express their thanks to the National Science Fund for General Projects (51874153) for the financial support of this research.

References

[1] P. Li, Y.L. Xie, Util. Miner. Resour., 4(2003) 13-16.

[2] F.F. Wu, Z.F. Cao, S. Wang, H. Zhong, J, J. Alloy. Compd., 722 (2017) 651-661.

[3] M. Ormran, T. Fabritius, A.M. Elmandy, N.A. Abdel-Khalek, S. Gornostayev, Sep. Purif. Technol., 156(2) (2015) 724-737.

[4] Y.B. Zhang, Z.J. Su, Y.L. Zhou, G.H. Li, T. Jiang, Int. J. Miner. Process., 124 (2013) 15-19.

[5] X.M. Zhang, Boiler Manuf., 4(2001) 42-44.

[6] Y. Yu, L. Li, J.Y. Wang, K.Z. Li, H.W, J. Alloy. Compd., 750 (2018) 8-16.

[7] L. Li, Z.J. Qiu, H. Wang, Y.G. Wei, B. Liao, X.L. SANG, Chin J Nonferrous Met., 24(2) (2014) 519-527.

[8] Y. Yu, L. Li, X.L. Sang, ISIJ Int., 56(1) (2016) 57-62.

[9] R.J. Zhang, L. Li, K.Z. Li, Y. Yu, ISIJ Int., 58 (3) (2018) 453-459.

[10] X.Y. Feng, L. Li, Y. Yu, X.L. SANG, Chin. J. Nonferrous Met., 26(9) (2016) 1990-1998.

[11] Y.B. Zhang, G.H. Li, T. Jiang, Y.F.Guo, Z.C. Huang, Int. J. Miner. Process., 110-111 (2012) 109-116.

[12] Y.B. Zhang, B.B. Liu, Z.J. Su, J. Chen, G.H. Li, T. Jiang, Int. J. Miner. Process., 144 (2015) 33-39.

[13] G.H. Li, Z.X. You, Y.B. Zhang, M.J. Rao, P.D. Wen, Y.F. Guo, T. Jiang, JOM., 66(9) (2014) 1701–1710.

[14] Y.B. Zhang, T. Jiang, G.H. Li, Z.C. Huang, Y.F. Guo, Ironmak Steelmak., 38(8) (2011) 613–619.

[15] Z.J. Su, Y.B. Zhang, B.B. Liu, Y.L. Zhou, T. Jiang, G.H. Li, Powder Technol., 292 (2016) 251-259.

[16] D.P. Tao, X.W. Yang, Chin. J. Nonferrous Met., 8(1) (1998), 126-130.

[17] Y. Li, S. H. Yang, C. B. Tang, Y. M. Chen, J. He, M.T. Tang, J. Min. Metall. Sect. B-Metall. 54 (1) B (2018) 73-79.

[18] S. Cahen, N. David, J.M. Fiorani, A. Maître, M.Vilasi, Thermochem. Acta., 403(2) (2003) 275-285.

[19] Y.B. Zhang, Z.J. Su, B.B. Liu, G.H. Li, Powder Technol., 292 (2016) 337 -343.

[20] X.Y. Xu, C. Hayes, E. Jak, Int. J. Mater. Res., 103 (2013) 529-536.

[21] B.S. Kim, J.C. Lee, H.S. Yoon, S.K. Kim, Mater. Trans., 2(9) (2011)1814 -1817.

[22] L.Y. Chen, Research on Separating Tin and Iron from Tin-bearing Iron Concentrate by Reduction Roasting Process, Central South University, Changshang, 2010, pp.1.

REDUKCIONO PONAŠANJE FAZE KOJA SADRŽI KALAJ U KONCENTRATU GVOŽĐA U PRISUSTVU MEŠAVINE GASOVA CO I CO_2

Y. Yu [a], H.-J. Li [*a,b], L. Li [a]

[a*] Glavna državna laboratorija za potpuno iskorišćenje resursa složenih obojenih metala, Inženjerski istraživački centar za očuvanje metalurške energije i smanjenje emisije pri Ministarstvu obrazovanja, Fakultet metalurškog i energetskog inženjerstva, Univerzitet nauke i tehnologije u Kunmingu, Kunming, Kina

[b] Institut za razvoj kvaliteta, Univerzitet nauke i tehnologije u Kunmingu, Kunming, Kina

Apstrakt

Osnovni cilj ovog istraživanja je bio da se utvrdi redukciono ponašanje faze koja sadrži kalaj (SnO_2) u koncentratu gvožđa koji sadrži kalaj na temeraturama od 1273 i 1373 K u prisustvu različitih koncentracija mešavine gasova CO i CO_2 putem hemijske analize, kao i XRD i SEM-EDS analiza. Rezultati pokazuju da redukciono ponašanje SnO_2 zavisi od temperature prženja i udela CO. Pri temperaturi od 1273 K, SnO_2 se redukuje do Sn (l), gde je udeo CO veći od 17,26 vol%, a SnO(s) se ne formira. Kada se temperatura poveća na 1373 K, SnO_2 se postepeno redukuje dok se ne formira $SnO_2 \rightarrow SnO\ (l) \rightarrow Sn(l)$ sa udelom CO većim od 15,75 vol%. Kinetička studija pokazuje da aktivaciona energija reakcije $SnO_2(s)+CO(g)=Sn(l)+\ CO_2(g)$ iznosi 144.75 kJ/mol na temperaturama od 1073-1223 K, što je niža vrednost od dobijene za redukciju $SnO_2(s)$ do SnO(g) pri temperaturama od 1273-1323 K. Na osnovu dobijenih rezultata se može doći do zaključka da kalaj prisutan u koncentartu gvožđa može efikasno da se ukloni nakon što se Sn(l) sulfurizuje u SnS na relativno niskim temperaturama (1073-1223 K) metodom sulfidnog prženja.

Ključne reči: *Redukciono ponašanje; SnO_2; Mešavina gasova CO i CO_2; Kinetika; Koncentarti gvožđa sa sadržajem kalaja*